

See discussions, stats, and author profiles for this publication at: <https://www.researchgate.net/publication/221805277>

# Effects of DNA Binding of the Zinc Finger and Linkers for Domain Fusion on the Catalytic Activity of Sequence-Specific Chimeric Recombinases Determined by a Facile Fluorescent Syst...

ARTICLE in BIOCHEMISTRY · FEBRUARY 2012

Impact Factor: 3.02 · DOI: 10.1021/bi201878x · Source: PubMed

---

CITATIONS

6

---

READS

14

8 AUTHORS, INCLUDING:



Wataru Nomura

Tokyo Medical and Dental University

60 PUBLICATIONS 483 CITATIONS

SEE PROFILE



Kenji Ohba

Hokkaido University

23 PUBLICATIONS 591 CITATIONS

SEE PROFILE

# Effects of DNA Binding of the Zinc Finger and Linkers for Domain Fusion on the Catalytic Activity of Sequence-Specific Chimeric Recombinases Determined by a Facile Fluorescent System

Wataru Nomura,<sup>\*,†</sup> Akemi Masuda,<sup>†,‡</sup> Kenji Ohba,<sup>§</sup> Arisa Urabe,<sup>†</sup> Nobutoshi Ito,<sup>‡</sup> Akihide Ryo,<sup>||</sup> Naoki Yamamoto,<sup>§</sup> and Hirokazu Tamamura<sup>\*,†,‡</sup>

<sup>†</sup>Institute of Biomaterials and Bioengineering, Tokyo Medical and Dental University, 2-3-10 Kandasurugadai, Chiyoda-ku, Tokyo 101-0062, Japan

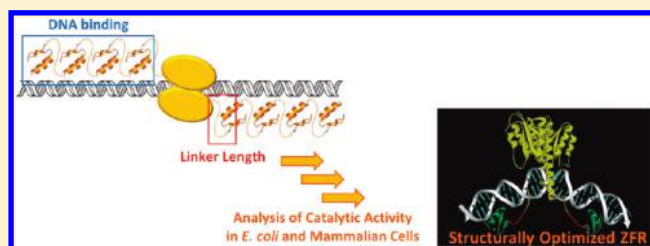
<sup>‡</sup>Graduate School of Biomedical Science, Tokyo Medical and Dental University, 1-45 Yushima, Bunkyo-ku, Tokyo 113-8510, Japan

<sup>§</sup>Department of Microbiology, Yong Loo Lin School of Medicine, National University of Singapore, Singapore 117597, Singapore

<sup>||</sup>Department of Microbiology and Molecular Biodefense Research, School of Medicine, Yokohama City University, 3-9 Fukuura, Kanazawa-ku, Yokohama 236-0004, Japan

## S Supporting Information

**ABSTRACT:** Artificial zinc finger proteins (ZFPs) consist of Cys<sub>2</sub>-His<sub>2</sub>-type modules composed of ~30 amino acids with a  $\beta\beta\alpha$  structure that coordinates a zinc ion. ZFPs that recognize specific DNA target sequences can substitute for the binding domains of enzymes that act on DNA to create designer enzymes with programmable sequence specificity. The most studied of these engineered enzymes are zinc finger nucleases (ZFNs). ZFNs have been widely used to model organisms and are currently in human clinical trials with an aim of therapeutic gene editing. Difficulties with ZFNs arise from unpredictable mutations caused by nonhomologous end joining and off-target DNA cleavage and mutagenesis. A more recent strategy that aims to address the shortcomings of ZFNs involves zinc finger recombinases (ZFRs). A thorough understanding of ZFRs and methods for their modification promises powerful new tools for gene manipulation in model organisms as well as in gene therapy. In an effort to design efficient and specific ZFRs, the effects of the DNA binding affinity of the zinc finger domains and the linker sequence between ZFPs and recombinase catalytic domains have been assessed. A plasmid system containing ZFR target sites was constructed for evaluation of catalytic activities of ZFRs with variable linker lengths and numbers of zinc finger modules. Recombination efficiencies were evaluated by restriction enzyme analysis of isolated plasmids after reaction in *Escherichia coli* and changes in EGFP fluorescence in mammalian cells. The results provide information relevant to the design of ZFRs that will be useful for sequence-specific genome modification.



Artificial zinc finger proteins (ZFPs) can be used to engineer DNA binding domains with high specificity for desired target sequences, and ZFPs are a promising technology for gene therapy.<sup>1–6</sup> Modular assembly of ZFPs can create a DNA binding domain that targets virtually any sequence in the human genome.<sup>3–5</sup> By linking ZFPs to the catalytic domains of DNA-modifying enzymes, novel enzymes, including nucleases,<sup>6</sup> recombinases,<sup>7–12</sup> and methylases,<sup>13–20</sup> have been fabricated. These enzymes are endowed with programmable DNA binding specificity provided by the zinc finger protein fusion. Relevant to our development of ZFRs, recombinase enzymes from the serine recombinase family have been well studied.<sup>21</sup> In comparison with members of the tyrosine recombinase family such as Cre and FLP recombinases, the serine recombinases, including Tn3 and  $\gamma\delta$  resolvases, Hin invertase, and Gin invertase, have DNA binding domains that are structurally independent of the catalytic domain. The structures of the catalytic domains and the sequences required for catalytic activity are highly conserved in these recombinases.<sup>22</sup> Tn3 and

$\gamma\delta$  are among the best-characterized site-specific recombinase enzymes in the serine recombinase family. Only 35 amino acid residues differ between the  $\gamma\delta$  and Tn3 resolvases, and their structures and functions are similar.<sup>23</sup> Negatively supercoiled DNA is a prerequisite for substrate recombination with native serine recombinase enzymes.<sup>21</sup> Although it is known that native serine recombinases require accessory proteins binding to sites I–III, activating mutants that require only the 28 bp of site I for successful recombination have been isolated.<sup>7</sup> In these hyperactivated enzymes, a DNA substrate in the form of negatively supercoiled DNA is not required for activity, and this allows application of activated catalytic domains with ZFPs to create zinc finger recombinases (ZFR). It has been suggested that reactions with serine recombinases proceed in three

**Received:** December 19, 2011

**Revised:** January 21, 2012

**Published:** January 23, 2012



steps: (i) formation of a dimer binding to the two forms of site I on the DNA, (ii) formation of a tetramer between the forms of site I, and (iii) strand exchange.<sup>24,25</sup> After the strand exchange reaction, the sequences between target sites are excised and the strands ligated (Figure 1).

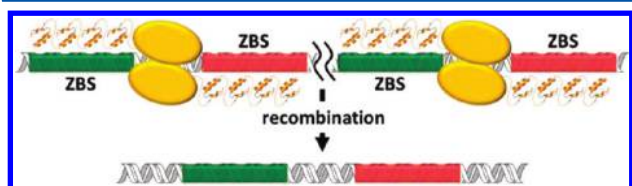


**Figure 1.** Schematic illustration of the ZFR reaction at a target site. The green and red boxes represent zinc finger binding sites (ZBSs). The yellow spheres represent catalytic domains of Tn3 resolvase.

ZFRs based on catalytic domain variants of Tn3, Gin, and Hin fused to artificial ZFPs have been shown to catalyze site-specific recombination in *Escherichia coli*<sup>7–11</sup> and mammalian cells.<sup>8,9,11,12</sup> ZFRs have also been shown to catalyze high-fidelity site-specific integration in mammalian cells.<sup>9,11,12</sup> While directed evolution of recombinase catalytic domains has proven to be essential for developing ZFR enzymes that function in mammalian cells, other aspects of ZFR design have not been thoroughly studied. In this report, we have synthesized ZFR mutants with variable numbers of zinc fingers and studied the role of peptide linkers that connect the Tn3 resolvase catalytic domain with the ZFP DNA binding domain. These effects are not readily addressed using molecular evolution strategies. For facile evaluation of recombination reactions in mammalian cells, a system that allows evaluation within 48 h was developed utilizing DsRed expression as a marker of transfection efficiency and EGFP expression as a marker of recombination efficiency. The results obtained revealed the optimal structures of the ZFRs, and the recombination efficiency results for linker mutants were verified by modeling studies.

## EXPERIMENTAL PROCEDURES

**Construction of ZFP Genes.** ZFP genes were constructed as described previously.<sup>26,27</sup> Briefly, plasmid pc3XB encoding ZFPs purchased from Addgene (<http://www.addgene.org>) was repeatedly ligated. The zinc finger gene that was obtained was inserted into pMAL-p4x as an *XbaI*–*BamHI* fragment for protein expression. A minor change was made to the multiple cloning site of pMAL-p4x (Figure S1 of the Supporting Information).

**Target Enzyme-Linked Immunosorbent Assays (ELISAs).** ELISA wells of 96-well plates were coated by incubation with 25  $\mu$ L of 8 ng/mL streptavidin in PBS for 1 h at 37 °C. The plates were washed twice with dH<sub>2</sub>O, and 25  $\mu$ L of 5'-biotinylated hairpin oligonucleotide target in zinc buffer A (ZBA) [10 mM Tris-HCl (pH 7.5), 90 mM KCl, 1 mM MgCl<sub>2</sub>, and 90  $\mu$ M ZnCl<sub>2</sub>] was added. After incubation for 1 h at 37 °C, plates were washed twice with dH<sub>2</sub>O. Blocking solution (ZBA with 3% BSA, 175  $\mu$ L) was added, and incubation continued for 1 h at 37 °C. The blocking solution was then removed; 25  $\mu$ L of purified protein in ZBA was added, and 2-fold serial dilutions were performed into 1% BSA, 5 mM DTT, and 10 ng/ $\mu$ L salmon sperm DNA in ZBA. After incubation for 1 h at room temperature, the plates were washed 10 times with dH<sub>2</sub>O and the monoclonal anti-MBP antibody (Sigma-Aldrich, 1:1000 dilution by ZBA with 1% BSA, 25  $\mu$ L) was added.

After incubation for 30 min at room temperature, the plates were washed 10 times with dH<sub>2</sub>O and a diluted secondary anti-mouse IgG AP conjugate (Sigma-Aldrich, 1:1000 dilution by ZBA with 1% BSA, 25  $\mu$ L) was added. After incubation for 30 min at room temperature, plates were washed 10 times with dH<sub>2</sub>O. The alkaline phosphatase reaction was performed with *p*-nitrophenylphosphate for 30 min, and the absorbance at 405 nm was read with a microplate reader. The data were collected and plotted. The data were fit to the equation  $y = 1/(1 + K_d/x)$ , where  $y$  is the proportion of bound MBP–ZFP fusion protein to maximal binding derived from the absorbance at 405 nm and  $x$  is the concentration of the MBP–ZFP fusion protein. The  $K_d$  values are averages of three or more independent experiments, and standard errors of the mean (SEM) are shown.

**Construction of ZFR Substrates.** Each substrate plasmid contained a recombination cassette composed of two ZFR recombination sites flanking an EGFP gene as a stuffer sequence. Cassettes were assembled by amplifying the EGFP gene with primers encoding the ZFR site. The polymerase chain reaction (PCR) product was cloned into pAra-OP.<sup>20</sup> ZFP genes were amplified by PCR from plasmid pc3XB and inserted into the plasmid as *EcoRI*–*SacI* fragments. Plasmids that contained ZFR with Gly-Ser linkers were mutated at the *BstBI* site before insertion of the catalytic domain.

**Construction of ZFR Genes.** The DNA fragment of the Tn3 resolvase catalytic domain was amplified from pWL625 (ATCC accession number 31787) utilizing 5'-GAGGAG-GAATTCATGCGACTTTTGGTTACGCT-3' and 5'-GAG-GAGAAGCTTTCACGAGGCCCTTTCGTCTT-3' as primers. The fragment was inserted into pBluescriptSK(–) as an *EcoRI*–*HindIII* fragment. Tn3-activating mutations (R2A, E56K, G101S, D102Y, M103I, and Q105L) were introduced into the Tn3 encoding gene. Linker sequences were amplified via PCR with the Tn3 fragment by primers that included the linker sequence. Tn3 fragments with different linkers were digested with *EcoRI* and *BglII* and ligated into similarly digested pAra-OP with the EGFP and ZFR sites. Tn3 fragments with various Gly-Ser linkers were also digested with *EcoRI* and *BstBI* and then ligated. The plasmids were maintained with chloramphenicol.

**Assay of Recombination of Plasmids in *E. coli*.** The plasmid with a ZFR gene downstream from the arabinose promoter and the substrate sequences were introduced into *E. coli* by electroporation. After incubation for 14 h at 37 °C on an LB-agar plate, colonies were picked up and grown for 14 h at 37 °C in LB medium. Purified plasmids were digested with *EcoRI* for 1 h at 37 °C. After electrophoresis on a 0.8% agarose gel, the fragment intensity was estimated with ImageJ (Figure S2 of the Supporting Information).

**Recombination Reaction of ZFR in Mammalian Cells.** The EGFP gene, flanked by recombination sites, was inserted between *NheI* and *KpnI* in pcDNAS/FRT (Life Technologies). A double-stranded oligonucleotide encoding the upstream target site was inserted into the *MluI* site, and the other oligonucleotide for the downstream target site was inserted into *KpnI* and *BamHI* sites. Cotransfection of the substrate plasmid and FLP expression plasmid (pOG44, Life Technologies) allowed site-specific integration into the single FLP recombinase target (FRT) site present in the FLP-In-CHO cell line (Life Technologies). Colony-acquired hygromycin resistance was characterized by fluorescently activated cell sorting (FACS) and genomic PCR. The sequence of the target site was confirmed. Cells were maintained in Ham's F-12 containing 10% (v/v)

Table 1. DNA Binding Affinities of ZFPs

	two fingers	three fingers	four fingers	five fingers	six fingers
$K_d$ (nM) <sup>a</sup>	160±20	23.6±3.6	12.8±1.1	15.4±1.4	12.9±1.4
$R^2$	0.90	0.87	0.94	0.94	0.94

<sup>a</sup>The values are averages of three or more independent experiments.

FBS and antibiotics (Wako Chemicals). The DsRed expression vector was constructed as follows; a DsRed-monomer sequence was ligated into pIRES2-EGFP (Clontech) to substitute for EGFP, and a Tn3-ZFP-NLS fragment was inserted between *NheI* and *EcoRI* in pIRES2-DsRed. On the following day, after  $2 \times 10^5$  cells had been seeded, the ZFR expression vector was transfected into cells using Lipofectamine LTX Reagent and PLUS Reagent (Life Technologies). After being transfected for 48 h, cells were collected and analyzed by flow cytometry.

## Molecular Modeling of the Linker Variants of ZFR.

Computer models were generated using Discovery Studio (Accelrys Inc.). The crystal structure of the  $\gamma\delta$  resolvase–DNA complex [Protein Data Bank (PDB) entry 1GDT]<sup>22</sup> was manually mutated in the protein and DNA to match the molecules used in this study. The first zinc finger module, obtained from a zinc finger–DNA complex (PDB entry 1MEY)<sup>28</sup> was placed on the resolvase–DNA complex by superimposing the phosphate backbone atoms of corresponding DNA residues. Appropriate linker atoms were then added and optimized by simulated annealing and energy minimization. During this optimization, the atoms in the resolvase, zinc fingers, and DNA were fixed, allowing only linker atoms to move.

## RESULTS

**Construction of Zinc Fingers and DNA Binding Analyses.** The 18 bp target sequence of the zinc finger protein utilized in this study was 5'-CTGCATGCACTGGATGCA-3'.

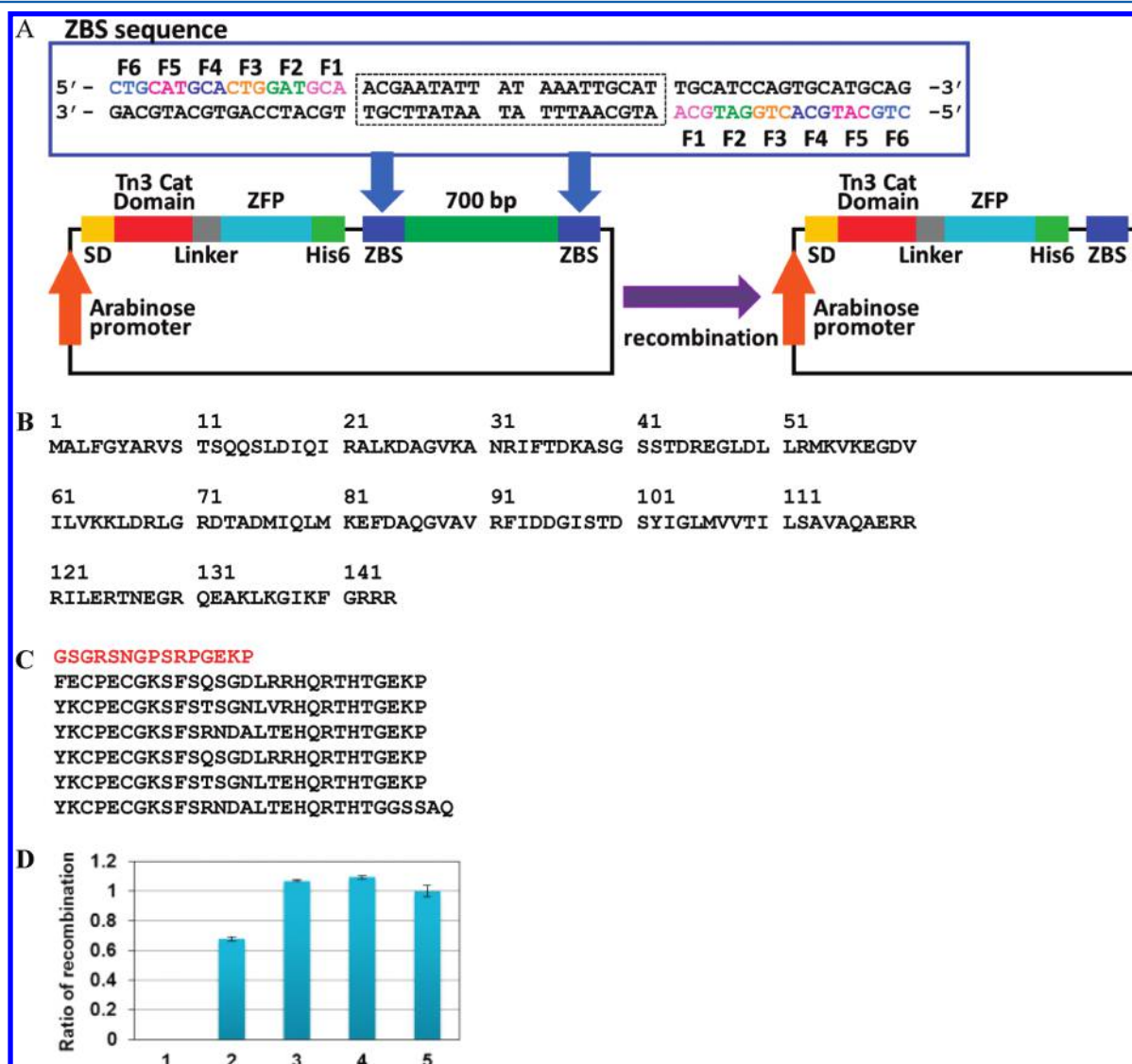


**Figure 2.** (A) Schematic of recombination at zinc finger binding sites (ZBSs). Recombination results in smaller plasmids. ZBS sequences are shown in the box. SD represents the Shine-Dalgarno sequence. (B) Amino acid sequences of the hyperactivated Tn3 catalytic domain. (C) Amino acid sequences of the linker (red) and six-zinc finger domain utilized for the analysis in *E. coli*. (D) Recombination efficiency depends on the number of fingers in ZFR. Columns 1–5 show the recombination efficiencies of two- through six-finger modules. The ratios are relative to the efficiency of the six-finger module. The error bars show the SEM of three or more independent experimental results.



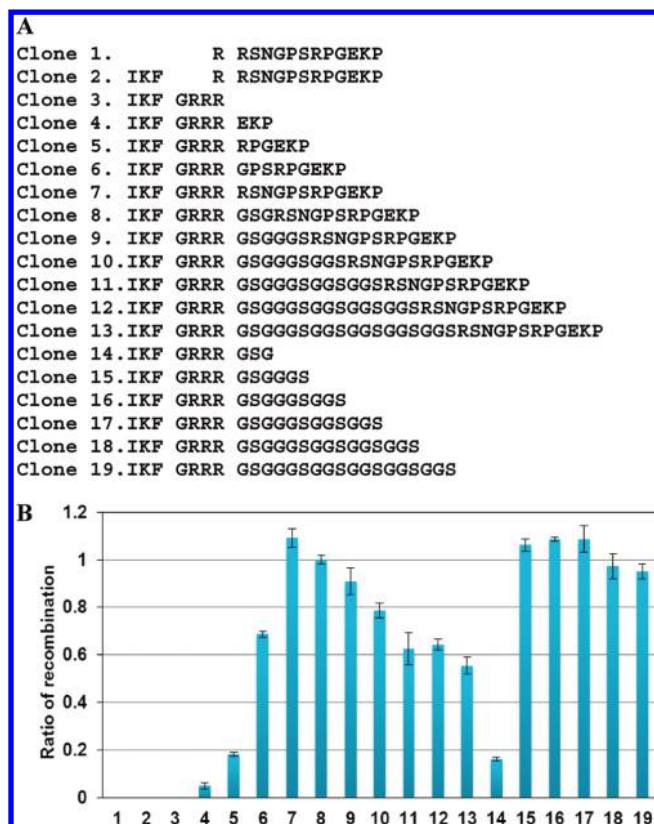


**Figure 3.** (A) Amino acid sequences of linkers of clones. All linkers were tested in the context of six-finger binding domains. (B) Results of recombination efficiency of clones with different linker sequences. The numbers of columns correspond to the clone numbers as described in panel A. The ratios are relative to the efficiency of clone 8. The error bars show the SEM of three or more independent experimental results.

Zinc fingers were constructed on the basis of a modular assembly strategy described by Barbas and co-workers.<sup>27,29–32</sup> Two- to six-finger proteins were constructed to obtain DNA binding domains with different affinities. Proteins were expressed as maltose binding protein fusions and purified with an MBPTrap column (GE Healthcare). The purity of the proteins was determined to be >90%. The DNA binding affinities were

evaluated by an ELISA with the biotinylated hairpin oligonucleotide as a target.<sup>10</sup> The binding constants ( $K_d$ ) of the two-, three-, four-, five-, and six-finger modules, listed in Table 1, were found to be 160, 23.6, 12.8, 15.4, and 12.9 nM, respectively. These results indicate that in the two-, three-, and four-finger modules, the DNA binding affinity increased with finger number but the binding affinities of ZFPs with four, five, and six fingers were similar.

**Construction of ZFR Chimeric Proteins and Recombination Analysis in *E. coli*.** The target DNA sequence of ZFR is shown in Figure 2A. The target site consists of a 20 bp spacer sequence flanked by 18 bp zinc finger binding sites. The spacer region was previously shown to be a Z+4 site in the target spacer of Z-resolvase.<sup>7</sup> For the evaluation of recombination in *E. coli*, a plasmid-based recombination system was constructed. The coding sequence of ZFRs was inserted into the plasmid containing a 700 bp stuffer sequence flanked with target sequences. In the recombination mediated by the expressed ZFRs, the stuffer sequence is excised to produce a smaller plasmid (Figure 2A). The amino acid sequences of the hyperactivated Tn3 catalytic domain, the linker between the domains, and the zinc finger domain are shown in panels B and C of Figure 2. The recombination efficiency was evaluated by a restriction enzyme assay. Plasmid purified from *E. coli* was digested by *EcoRI*, which is a single cutter of the plasmid. The linear plasmid was analyzed on an 0.8% agarose gel, and the fractions of the longer (nonrecombinant) and shorter (recombinant) plasmids were evaluated (Figure S2 of the Supporting Information). ZFR variants with different numbers of fingers were evaluated in this recombination system, and recombination ratios increased with increasing numbers of fingers from two to four fingers. The values of recombination efficiencies for ZFRs with four to six fingers were similar, reflecting the DNA binding affinities (Figure 2D). The production of recombinant sequence was confirmed by DNA sequencing analysis (Figure S3 of the Supporting Information).

In the next study, the reactions of ZFR variants with different linker lengths in the context of the six-finger module were tested (Figure 3B). In this experiment, 19 constructs were prepared. The variants were categorized into three groups depending on lengths and the compositions of linker sequences. The first group variants have short linkers with deletions within the catalytic

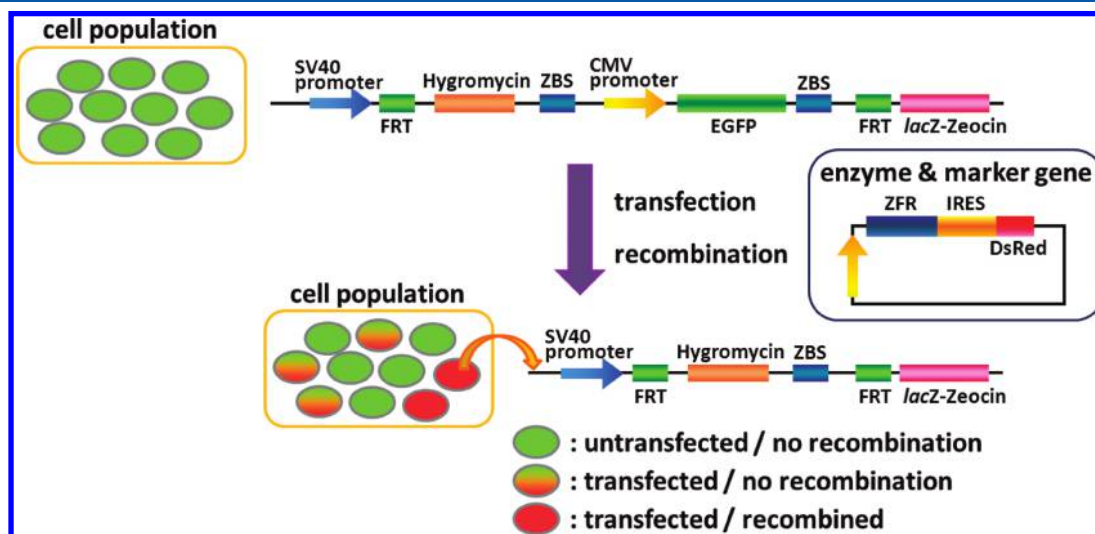


**Figure 4.** Recombination system constructed utilizing FLP-In-CHO-K1 cells.

domain of Tn3 resolvase (clones 1 and 2). The second group of variants has semirigid linkers (clones 3–13). The third group has flexible linker sequences composed of Gly-Ser sequences (clones 14–19). In the clones of the third group, the first two amino acids of the zinc finger domain, Tyr and Lys, are substituted with Phe and Glu, respectively. The recombination efficiencies were determined in the *E. coli*-based assay (Figure 3B). The results indicate two important phenomena. (1) The variant with a 12-amino acid linker was the most efficient (clone 7, Figure 3A), suggesting that there is an optimal linker length. (2) The variants with linkers composed of only Gly-Ser sequences were most efficient (clones 15–17, Figure 3A), indicating that ZFRs with flexible linkers tended to recombine most efficiently.

#### ZFR-Catalyzed Recombination in Mammalian Cells.

To evaluate the recombination efficiency of ZFR variants in mammalian cells, we constructed a reporter cell line from Flp-In-CHO-K1 containing a cassette that encodes EGFP driven by a CMV promoter flanked by target sites (Figure 4). As each cell contains a single copy of the reporter gene, the recombination efficiency can be calculated from the proportion of cells with or without EGFP fluorescence. Additionally, the expression of ZFR was monitored by the expression of DsRed; this gene was placed downstream of the ZFR gene via a IRES sequence. The genes encoding ZFRs utilized in this study were amplified from a pAra plasmid shown in Figure 2A. Thus, the sequences of clones are the same as those utilized in experiments in *E. coli*.

With this reporter system, recombination efficiencies could be evaluated 48 h after transfection. Reported procedures involving retroviral-based transduction, selection, and evaluation take nearly 10 days.<sup>8</sup> The fluorescence intensity of cells was detected by FACS analysis (Figure S4 of the Supporting Information). The cells with recombinant genes were those that were EGFP-negative and DsRed-positive. The recombination efficiencies depended on the number of finger modules and on the linker lengths (Figure 5). As in *E. coli*, the five-finger proteins were the most efficient in recombination. The optimal linker length was six residues, which is different from that in *E. coli*. Additionally, recombination in mammalian cells was not as efficient as that in *E. coli*.

## DISCUSSION

This study demonstrated that ZFR recombinases can be designed to specifically target sites in *E. coli* and mammalian cells and that recombination efficiency depends on the affinity of the ZFP for the DNA target and on the length of the linker between the DNA binding domain and the recombinase domain. The ZFR with five fingers had the highest recombination efficiency in both *E. coli* and CHO-K1 cells. The DNA binding affinity of this particular ZFP was saturated when the DNA binding domain had more than five fingers. The association and dissociation with DNA binding depend on the number of finger modules.<sup>33</sup> It is possible that the ZFR with five fingers was the most efficient recombination because the balance of association with dissociation and turnover was optimal. Guo et al. have also reported that four and five ZF domains are optimal for activity of ZFN.<sup>34</sup> On the basis of our data, the apparent  $K_d$  values of the four-, five-, and six-finger proteins derived from this particular ZFP were similar. The dependence on the number of finger modules was common in both *E. coli* and mammalian cells, but the recombination efficiency was lower in mammalian cells. In CHO-K1 cells, DNA is sequestered in chromatin structures. Additionally, the

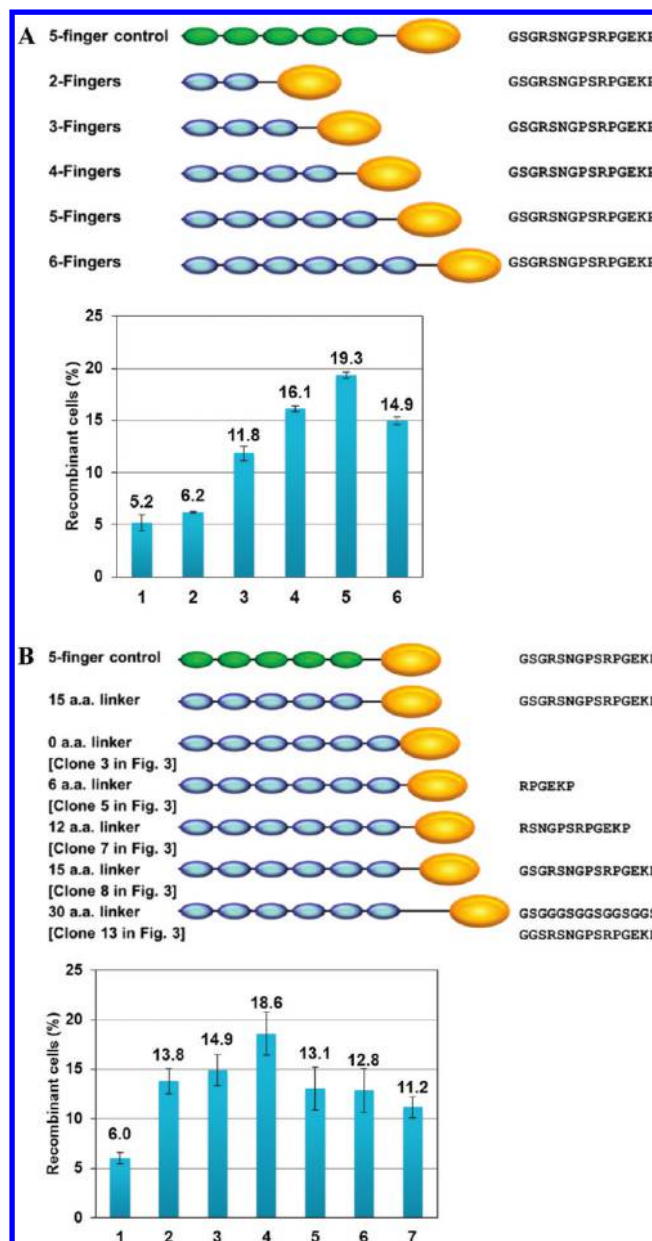


**Figure 5.** Recombination efficiency of ZFRs containing various numbers of fingers (A) and with various linkers (B) in mammalian cells. The top cartoons represent ZFR constructs utilized in the analyses. Green, blue, and yellow spheres represent zinc finger modules without sequence specificity, zinc finger modules with sequence specificity, and the Tn3 catalytic domain, respectively. Letters at the right of the cartoons are the linker sequences of the constructs. (A) Dependence on the number of fingers of ZFRs. The columns are as follows: column 1, five-finger control (nonspecific DNA binding); column 2, two fingers; column 3, three fingers; column 4, four fingers; column 5, five fingers; column 6, six fingers and different linker lengths. (B) Dependence on linker length. The columns are as follows: column 1, nontarget five-finger control with 15 amino acids; column 2, targeted five-finger ZFR with 15-amino acid linker; columns 3–7, targeted six-finger ZFRs with linker lengths of 0, 6, 12, 15, and 30 amino acids, respectively. The error bars show the SEM of three or more independent experimental results.

circular form of plasmid DNA could enhance recombination in the bacterial cells.

Recombination efficiency was dependent on the linker between the zinc finger domain and the recombinase domain. ZFRs with the shortest linkers had a very low efficiency of



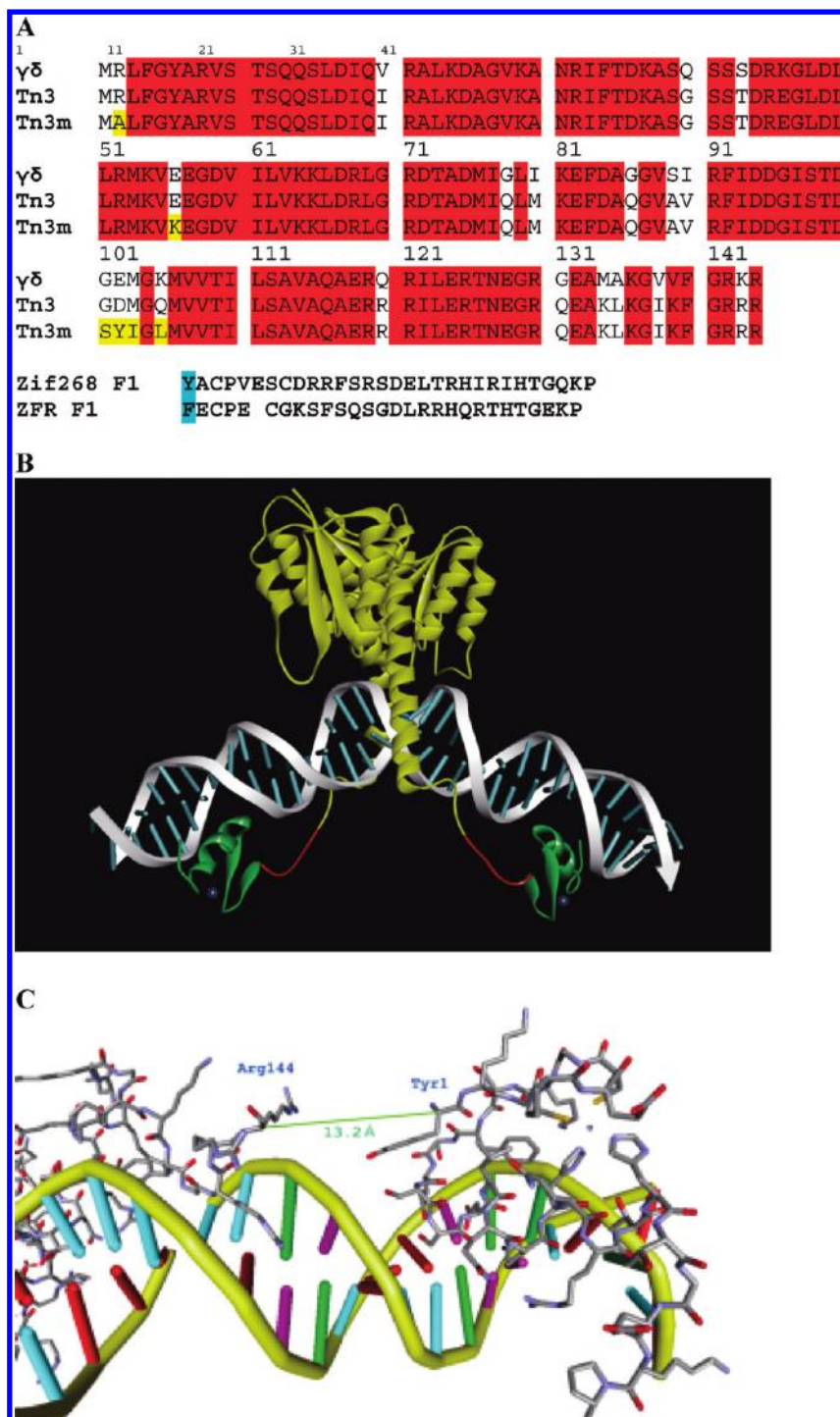


**Figure 6.** Representative result of molecular modeling of the resolvase domain and the first zinc finger module separated by a six-amino acid linker sequence. (A) Sequence alignment of resolvases  $\gamma\delta$  and Tn3 and the Tn3 hyperactivated mutant (Tn3m) (top), the first finger of zif268, and ZFR. Conserved residues are highlighted in red, and amino acid substitutions in the hyperactive mutant are highlighted in yellow. The N-terminal aromatic amino acids of zinc fingers are highlighted in blue. (B) The yellow ribbon indicates  $\gamma\delta$  resolvase, the red ribbon the six-amino acid linker, the green ribbon the N-terminal zinc finger domain, and the gray ribbon the zinc ion. (C) Distances between  $\text{Ca}$  atoms of Arg144 and tyrosine (Tyr) at the N-terminus of zif268. The N-terminal amino acid of the zinc finger domain is phenylalanine (Phe) in ZFRs utilized in this study.

recombination in both bacterial and mammalian cells. Second, the length of linkers based on the original sequences was critical. Proteins with linkers containing 12 amino acid residues were the most efficient in recombination. In the Gly-Ser linker variants, the recombination efficiency reached a maximum at six amino acids. This result indicates that both the length and the flexibility of the linker are important.

A molecular modeling study was performed in an attempt to assess the reasons for the differences in recombination efficiency among the linker mutants. In the modeling of the ZFR complex with target DNA, the linker length of six amino acids was optimal for the DNA binding of ZFR when the linker sequence was flexible (Figure 6A). When the domains were modeled bound to the target sequence, the distance between

the C $\alpha$  atom of Arg144 in the  $\gamma\delta$  resolvase (Figure S5 of the Supporting Information) and that of Tyr at the N-terminus of the zinc finger domain is  $\sim 13.2$  Å (Figure 6B,C). In polypeptides in the extended conformation, the distance between C $\alpha$  atoms of sequential amino acids is 3.8 Å. Thus, a linker consisting of three amino acids (clone 4 or clone 14) should allow the protein to bind to both DNA regions, although these ZFRs had very low recombination efficiencies. In the complex with DNA, the amino groups at positions 145 and 146 of the main chain in  $\gamma\delta$  resolvase interact with the phosphate backbone of DNA and amino acids of these positions are involved in the folding of the catalytic domain (Figure S5 of the Supporting Information). In the case of clone 4, the Lys-Pro residues at the C-terminus of linker residues are involved in the folding of the zinc finger domain. Thus, these amino acids are considered to be members of both domains, not of the linker sequences. With this reasoning, the six and nine amino acids in the linkers for clones 4 and 5, respectively, are shorter than the theoretically optimal length. Moreover, in the sequences of the six- and nine-amino acid linkers, the amino acid at position 146 is Pro, which could disrupt the interaction with DNA phosphate, thus lowering the recombination efficiency. Consistent with these estimations, the Gly-Ser linker with six or nine amino acids (clones 15 and 16, respectively) showed the best recombination ratio. This evidence indicates that the residues at the C-terminus of the catalytic domain and the N-terminus of the zinc finger domain are involved in domain folding because Lys-Pro residues at the N-terminus of the zinc finger domains are not included in these clones. Variants around this optimal linker length, especially those with 12 and 15 amino acids, had similar recombination efficiencies. These results show that the flexibility of the linker is not necessary when the linker length is optimal. In mammalian cells, the variant with a linker of six amino acids (clone 5) showed the best recombination and the zero-amino acid linker (clone 3) showed better recombination than the variants with longer linkers of more than 12 amino acids. The reason for this effect is unclear, but it could be due to differences in the structures of target sites on the plasmid DNA compared to the genomic DNA. Additionally, the distances between the binding sites in these systems are different. In the genomic target, the binding sites are separated by sequences of more than 2500 bp.

In this study, a newly developed recombination system allowed measurement of recombination efficiencies of ZFRs in *E. coli* and in mammalian cells. In mammalian cells, recombination with genomic targets was evaluated within 48 h of the transient expression of recombinases. Artificial enzymes such as ZFN and ZFR have been studied mainly by using viral vector systems to deliver their genes into mammalian genomes. In a report describing utilization of the retrovirus vectors for gene delivery, the recombination efficiency was as high as  $\sim 18\%$ .<sup>8</sup> In our study, we also observed up to 18% recombination in cells. This system could be utilized in future studies to evaluate function of ZFRs on specific targets.

## ■ ASSOCIATED CONTENT

### ■ Supporting Information

Details of subcloning, experimental results of plasmid digestion and sequencing, results of FACS analyses, and a description of key interactions in  $\gamma\delta$  resolvase. This material is available free of charge via the Internet at <http://pubs.acs.org>.

## ■ AUTHOR INFORMATION

### Corresponding Author

\*E-mail: [nomura.mr@tmd.ac.jp](mailto:nomura.mr@tmd.ac.jp) or [tamamura.mr@tmd.ac.jp](mailto:tamamura.mr@tmd.ac.jp).  
Phone: +81-3-5280-8036. Fax: +81-3-5280-8039.

### Funding

This work was supported in part by a Grant-in-Aid for Scientific Research from the Ministry of Education, Culture, Sports, Science and Technology, Japan (20790060), Health and Labor Sciences Research Grants from the Japanese Ministry of Health, Labor, and Welfare, and a grant from the Mochida Memorial Foundation for Medical and Pharmaceutical Research to W.N.

### Notes

The authors declare no competing financial interest.

## ■ REFERENCES

- (1) Beerli, R. R., Dreier, B., and Barbas, C. F. III (2000) Positive and negative regulation of endogenous genes by designed transcription factors. *Proc. Natl. Acad. Sci. U.S.A.* 97, 1495–1500.
- (2) Pabo, C. O., Peisach, E., and Grant, R. A. (2001) Design and selection of novel Cys2His2 zinc-finger proteins. *Annu. Rev. Biochem.* 70, 313–340.
- (3) Beerli, R. R., and Barbas, C. F. III (2002) Engineering polydactyl zinc-finger transcription factors. *Nat. Biotechnol.* 20, 135–141.
- (4) Jamieson, A. C., Miller, J. C., and Pabo, C. O. (2003) Drug discovery with engineered zinc-finger proteins. *Nat. Rev. Drug Discovery* 2, 361–368.
- (5) Blancafort, P., Segal, D. J., and Barbas, C. F. III (2004) Designing transcription factor architectures for drug discovery. *Mol. Pharmacol.* 66, 1361–1371.
- (6) Carroll, D. (2008) Progress and prospects: Zinc-finger nucleases as gene therapy agents. *Gene Ther.* 15, 1463–1468.
- (7) Akopian, A., He, J., Boockvar, M. R., and Stark, W. M. (2003) Chimeric recombinases with designed DNA sequence recognition. *Proc. Natl. Acad. Sci. U.S.A.* 100, 8688–8691.
- (8) Gordley, R. M., Smith, J. D., Gräslund, T., and Barbas, C. F. III (2007) Evolution of programmable zinc-finger-recombinases with activity in human cells. *J. Mol. Biol.* 367, 802–813.
- (9) Gordley, R. M., Gersbach, C. A., and Barbas, C. F. III (2009) Synthesis of programmable integrases. *Proc. Natl. Acad. Sci. U.S.A.* 106, 5053–5058.
- (10) Gersbach, C. A., Gaj, T., Gordley, R. M., and Barbas, C. F. III (2010) Directed evolution of recombinase specificity by split gene reassembly. *Nucleic Acids Res.* 38, 4198–4206.
- (11) Gaj, T., Mercer, A. C., Gersbach, C. A., Gordley, R. M., and Barbas, C. F. III (2011) Structure-Guided Reprogramming of Serine Recombinase DNA Sequence Specificity. *Proc. Natl. Acad. Sci. U.S.A.* 108, 498–503.
- (12) Gersbach, C. A., Gaj, T., Gordley, R. M., Mercer, A. C., and Barbas, C. F. III (2011) Targeted plasmid integration into the human genome by an engineered zinc-finger recombinase. *Nucleic Acids Res.* 39, 7868–7878.
- (13) Xu, G.-L., and Bestor, T. H. (1997) Cytosine methylation targeted to predetermined sequences. *Nat. Genet.* 17, 376–378.
- (14) McNamara, A. R., Hurd, P. J., Smith, A. E., and Ford, K. G. (2002) Characterisation of site-biased DNA methyltransferases: Specificity, affinity and subsite relationships. *Nucleic Acids Res.* 30, 3818–3130.
- (15) Carvin, C. D., Parr, R. D., and Kladde, M. P. (2003) Site-selective in vivo targeting of cytosine-5 DNA methylation by zinc-finger proteins. *Nucleic Acids Res.* 31, 6493–6501.
- (16) Minczuk, M., Papworth, M. A., Kolasinska, P., Murphy, M. P., and Klug, A. (2006) Sequence-specific modification of mitochondrial DNA using a chimeric zinc-finger methylase. *Proc. Natl. Acad. Sci. U.S.A.* 103, 19689–19694.
- (17) Li, F., Papworth, M., Minczuk, M., Rohde, C., Zhang, Y., Ragozin, S., and Jeltsch, A. (2007) Chimeric DNA methyltransferases



target DNA methylation to specific DNA sequences and repress expression of target genes. *Nucleic Acids Res.* 35, 100–112.

(18) Smith, A. E., and Ford, K. G. (2007) Specific targeting of cytosine methylation to DNA sequences in vivo. *Nucleic Acids Res.* 35, 740–754.

(19) Smith, A. E., Hurd, P. J., Bannister, A. J., Kouzarides, T., and Ford, K. G. (2008) Heritable Gene Repression through the Action of a Directed DNA Methyltransferase at a Chromosomal Locus. *J. Biol. Chem.* 283, 9878–9885.

(20) Nomura, W., and Barbas, C. F. III (2007) In vivo site-specific DNA methylation with a designed sequence-enabled DNA methylase. *J. Am. Chem. Soc.* 129, 8676–8677.

(21) Grindley, N. D., Whiteson, K. L., and Rice, P. A. (2006) Mechanisms of site-specific recombination. *Annu. Rev. Biochem.* 75, 567–605.

(22) Yang, W., and Steitz, T. A. (1995) Crystal structure of the site-specific recombinase gamma delta resolvase complexed with a 34 bp cleavage site. *Cell* 82, 193–207.

(23) Arnold, P. H., Blake, D. G., Grindley, N. D., Boocock, M. R., and Stark, W. M. (1999) Mutants of Tn3 resolvase which do not require accessory binding sites for recombination activity. *EMBO J.* 18, 1407–1414.

(24) Li, W., Kamtekar, S., Xiong, Y., Sarkis, G. J., Grindley, N. D., and Steitz, T. A. (2005) Structure of a synaptic  $\gamma\delta$  resolvase tetramer covalently linked to two cleaved DNAs. *Science* 309, 1210–1215.

(25) Olorunniji, F. J., He, J., Wenwieser, S. V., Boocock, M. R., and Stark, W. M. (2008) Synapsis and catalysis by activated Tn3 resolvase mutants. *Nucleic Acids Res.* 36, 7181–7191.

(26) Gonzalez, B., Schwimmer, L. J., Fuller, R. P., Ye, Y., Asawapornmongkol, L., and Barbas, C. F. III (2010) Modular system for the construction of zinc-finger libraries and proteins. *Nat. Protoc.* 5, 791–810.

(27) Mandell, J. G., and Barbas, C. F. III (2006) Zinc Finger Tools: Custom DNA-binding domains for transcription factors and nucleases. *Nucleic Acids Res.* 34, W516–W523.

(28) Kim, C. A., and Berg, J. M. (1996) A 2.2 Angstroms resolution crystal structure of a designed zinc finger protein bound to DNA. *Nat. Struct. Mol. Biol.* 3, 940–945.

(29) Segal, D. J., Dreier, B., Beerli, R. R., and Barbas, C. F. III (1999) Toward controlling gene expression at will: Selection and design of zinc finger domains recognizing each of the 5'-GNN-3' DNA target sequences. *Proc. Natl. Acad. Sci. U.S.A.* 96, 2758–2763.

(30) Dreier, B., Segal, D. J., and Barbas, C. F. III (2000) Insights into the molecular recognition of the 5'-GNN-3' family of DNA sequences by zinc-finger domains. *J. Mol. Biol.* 303, 489–502.

(31) Dreier, B., Beerli, R. R., Segal, D. J., Flippin, J. D., and Barbas, C. F. III (2001) Development of zinc finger domains for recognition of the 5'-ANN-3' family of DNA sequences and their use in the construction of artificial transcription factors. *J. Biol. Chem.* 276, 29466–29478.

(32) Dreier, B., Fuller, R. P., Segal, D. J., Lund, C., Blancafort, P., Huber, A., Koksche, B., and Barbas, C. F. III (2005) Development of zinc finger domains for recognition of the 5'-CNN-3' family DNA sequences and their use in the construction of artificial transcription factors. *J. Biol. Chem.* 280, 35588–35597.

(33) Kamiuchi, T., Abe, E., Imanishi, M., Kaji, T., Nagaoka, M., and Sugiura, Y. (1998) Artificial nine zinc-finger peptide with 30 base pair binding sites. *Biochemistry* 37, 13827–13834.

(34) Guo, J., Gaj, T., and Barbas, C. F. III (2010) Directed evolution of an enhanced and highly efficient FokI cleavage domain for zinc finger nuclease. *J. Mol. Biol.* 400, 96–107.